J Mol Model (2013) 19:3065–3075
DOI 10.1007/s00894-013-1831-y

ORIGINAL PAPER

Density functional study of structural and electronic properties of small binary Be_nCu_m ($n+m=2\sim7$) clusters

Si-Cheng Li · Ying Li · Di Wu · Zhi-Ru Li

Received: 23 September 2012 / Accepted: 19 March 2013 / Published online: 14 April 2013

Abstract The geometrical structures, electronic properties and relative stabilities of small bimetallic Be_nCu_m ($n+m=2$–7) clusters have been systematically investigated by using a density functional method at the B3PW91 level. In the most stable structures of Be_nCu_m, the Be atoms tend to gather together and construct similar configurations to those of pure Be_n clusters. Meanwhile, there is a tendency for Cu atoms to segregate toward the Be_n cluster surface. The successive binding energies, cohesive energies, second difference of energies, the highest occupied-lowest unoccupied molecular orbital energy gaps and chemical hardness of Be_nCu_m are also investigated. All of them demonstrate that the clusters with even number of copper atoms present relatively higher stabilities. The natural population analyses on the Be_nCu_m clusters reveal that, the charge transfers from Be to Cu when the average coordination numbers (Nc) of Be atom is less than 3, whereas the charge-transferring direction reverses when Nc(Be) increases.

Keywords Be-Cu cluster · Coordination number · Density functional theory · Stability · Structural feature

Introduction

Over the past decades, a lot of emphases have been put on the study of the physical and chemical properties of atomic clusters, which, consisting of a few to a few thousand atoms, have come to be regarded as a new "phase" of matter. Interestingly, the characteristics of atomic clusters, such as geometrical arrangements and electronic properties, can be tuned up by altering the clusters' size and composition, which are generally inaccessible in the bulk phase. Among the various studies on clusters, metal clusters, especially the bimetallic clusters, have attracted considerable attention from both experimental and theoretical researchers [1–17]. The goal of most of these studies is to examine how the properties of a cluster evolve with size. These properties include the geometric structures, binding energies, ionization energies, and the highest occupied-lowest unoccupied molecular orbital (HOMO-LUMO) energy gaps, etc.

Beryllium copper (BeCu) alloys are known for their high strength and good electrical and thermal conductivities. They have many specialized applications in tools for hazardous environments, aerospace, and precision measurement devices, etc. In view of the practical importance of beryllium copper alloys in our life, the investigations on the Be-Cu systems are intriguing and may help to understand various physical and chemical properties and stabilities of such species. However, although much of the experimental and theoretical work has been carried out on pure beryllium [18–33] and copper [34–44] clusters, there is limited theoretical research on the binary clusters of Be/Cu. Thus, characterization of geometrical structures, various energetic and electronic-structure related properties of the Be-Cu clusters should be a meaningful project. Such a study on the Be-Cu clusters would also provide useful information on how their geometrical arrangements and stabilities evolve with varying cluster size and composition.

In this paper, we present a systematic study of the bimetallic Be_nCu_m ($n+m\leq7$) clusters at their neutral states. Compared to pure Be_n and Cu_m clusters, the Be_nCu_m binary clusters exhibit some interesting structural evolutions. The successive binding energy (sBE) of Be_nCu_m shows odd-even oscillations. The stabilities of the Be_nCu_m clusters are analyzed on the basis of the vertical ionization potentials

S.-C. Li · Y. Li · D. Wu (✉) · Z.-R. Li
Institute of Theoretical Chemistry, State Key Laboratory of Theoretical and Computational Chemistry, Jilin University, Changchun 130023, People's Republic of China
e-mail: wud@mail.jlu.edu.cn

(IP_v), the cohesive energies (E_C), the HOMO-LUMO gaps, the chemical hardness and the second difference energies. In addition, the natural population analyses (NPA) are performed to figure out the charge-transfer direction in the Be_nCu_m clusters.

Calculation methods

The randomized algorithms [45–48] were used to search the minimum structures of the Be_nCu_m ($n+m\leq7$) clusters. In this method, all atoms were placed at a common initial point in geometrical space and then exploded in random directions within a sphere-shell with radius between R_{min} and R_{max}. Such "zero" input structure can avoid biasing the search. A lot of starting geometries were obtained at the B3LYP/LANL2DZ level until no new minimum appeared. Afterward, randomized searches were implemented again in the region of one structure found above to do an intensive search for additional minima. The minima at the B3LYP/LANL2DZ level were then reoptimized using the B3PW91 method [49]. In the reoptimization, the SDD [50] and aug-cc-pVTZ basis sets were adopted for Cu and Be, respectively. In order to make sure that the lowest energetic structures are obtained, we have also considered a large amount of initial Be_nCu_m geometries based on the pure copper or beryllium clusters. For example, the $BeCu_m$ structures can be constructed by placing a beryllium atom on each possible site of the Cu_m cluster, or by substituting one Cu atom in the Cu_{m+1} cluster with a Be atom. Finally, B3PW91 frequency calculations (with SDD basis set for Cu and aug-cc-pVTZ for Be) were performed on all the optimized Be_nCu_m structures to check whether they were transition states or true minima on the potential energy surfaces.

To evaluate the feasibility of our method, we make a comparison between the calculated structures of the Cu_2 and Be_2 dimers and those from experimental works [24, 51, 52]. The results of bond lengths and vibrational frequencies are summarized in Table 1. From the table, the B3PW91 method yields $R_{Be\text{-}Be}$=2.491 Å and $R_{Cu\text{-}Cu}$=2.235 Å, which are in good agreement with the corresponding experimental data of 2.453 Å and 2.22 Å, respectively. Meanwhile, the B3LYP results also agree well with those from experiment. In view of the fact that the B3PW91 method has been reported to perform satisfactorily on characterizing structures and stabilities of pure Be clusters [26, 28], bare Cu clusters [53], and binary Be_nC_m clusters [54], we adopt the B3PW91 method in final optimizations of the Be_nCu_m geometries.

All the single-point energy calculations were carried out at the B3PW91 level with SDD basis set for Cu and aug-cc-pVTZ for Be. Based on the single-point energies, the vertical ionization potentials (IP_v), the HOMO-LUMO energy gaps, the successive binding energy (sBE), the cohesive energies (E_C), the chemical hardness and the second difference energies of Be_nCu_m were obtained. Natural population analyses (NPA) [55, 56] were implemented at the same level to give natural atomic charges distribution. All calculations were performed using the GAUSSIAN 09 program package[57].

Results and discussion

Structural characteristics

The lowest energy structures of the Be_nCu_m ($n+m\leq7$) clusters are shown in Fig. 1, their symmetries and lowest vibrational frequencies are presented in Table 2. The geometrical parameters of these structures are collected in Table 3. In this subsection, we will discuss the structures of the Be_nCu_m clusters according to the increasing order of n.

1. *$BeCu_m$ ($m=1–6$)*. Among the six clusters in this group, there are two clusters that show linear structures, namely, BeCu and $BeCu_2$; two are planar, i.e., $BeCu_3$ and $BeCu_4$; and the other two, $BeCu_5$ and $BeCu_6$, present 3-dimensional (3D) geometries. Note that the Be-doped Cu_m clusters exhibit different structural features from the pure copper clusters. It is known that the structures of Cu_m (m=3–6) are all planar [53], while in the $BeCu_m$ series, the 3D structure occurs at m=5.

In the case of BeCu with $C_{\infty v}$ symmetry, the Be-Cu bond length is 2.057 Å, which is shorter than Be-Be bond length (2.453 Å[24]) in Be dimer and Cu-Cu bond length (2.491 Å) in Cu_2. For $BeCu_2$ with $D_{\infty h}$ symmetry, the Be-Cu bond length is 2.044 Å, which is slightly shorter than that of BeCu. The global minimum of $BeCu_3$, exhibits a quasi-rhombic structure with C_{2v} symmetry. From Table 3, the Cu-Cu bond lengths are 2.426 Å, which are shorter than that of Cu_2 (2.491 Å); the axial Be-Cu bond length is 2.126 Å, which is slightly longer than the Be1-Cu2 bond length of 2.093 Å. This cluster could be regarded as a copper atom in Cu_4[53] being replaced by a beryllium atom. The optimized geometry of $BeCu_4$ has a C_{2v} geometrical symmetry. In comparison with the bare Cu_5 cluster[53], $BeCu_4$ could be obtained by substituting a Be atom for the central Cu atom in Cu_5, with the configuration having a slight deformation. The next one is $BeCu_5$, which is the first 3D structure in this group and exhibits an umbrella-like geometry. The Be1-Cu2 bond length of 2.129 Å is slightly shorter than that of 2.142 Å for Be1-Cu3 bond. As a result, the $BeCu_5$ cluster has C_s spatial symmetry. The Cu-Cu bond lengths have

Table 1 Comparison of calculated and experimental bond lengths (R in Å) and vibrational frequencies (ν in cm^{-1}) of pure beryllium and copper dimers

Methods	Be_2		Methods	Cu_2	
	R	ν		R	ν
B3PW91/aug-cc-pVTZ	2.491	300.35	B3PW91/SDD	2.235	264.80
B3LYP/aug-cc-pVTZ	2.482	287.27	B3LYP/SDD	2.245	259.48
Experimental[a]	2.453	270.7	Experimental	2.22[b,c]	265[c]

[a]from ref [24], [b]from ref [51], [c]from ref [52]

three different values, namely, 2.411 Å for bond 5–6, 2.516 Å for bond 3–5, and 2.493 Å for bond 3–6. The last cluster in this group is $BeCu_6$ with C_{3v} symmetry.

From Fig. 1, each $BeCu_m$ structure can be gained by adding a Cu atom on the geometry of the former $BeCu_{m-1}$ cluster. Besides, the introduction of one more Cu atom influences the $BeCu_{m-1}$ geometry in an interesting way. Specifically, if a Cu′ atom in $BeCu_{m-1}$ bonds with the added Cu atom, then the Cu′-Be bond will elongate; if not, the Cu′-Be bond will shorten. Take Be1-Cu2 bond for example, the Cu2 atom does not connect with the Cu3 atom, so the addition of Cu3 atom to BeCu leads to a shorter Be1-Cu2 bond (from 2.057 to 2.044 Å). Likewise, the same is true for the introduction of Cu5 or Cu7 atom, which reduces the Be1-Cu2 bond length from 2.093 to 2.080 Å and from 2.129 to 2.114 Å, respectively. In contrast, both Cu4 and Cu6 atoms link with Cu2 atom, as a result, the Be1-Cu2 bond becomes longer from 2.044 Å in $BeCu_2$ to 2.093 Å in $BeCu_3$ and from 2.080 Å in $BeCu_4$ to 2.129 Å in $BeCu_5$.

2. *Be_2Cu_m* (*m=1–5*). When two beryllium atoms are involved in these binary clusters, the 3D geometry occurs at m=3. For the $C_{\infty v}$ -symmetrical Be_2Cu, the Be-Cu bond length is 2.044 Å, which is the same with that in $BeCu_2$.

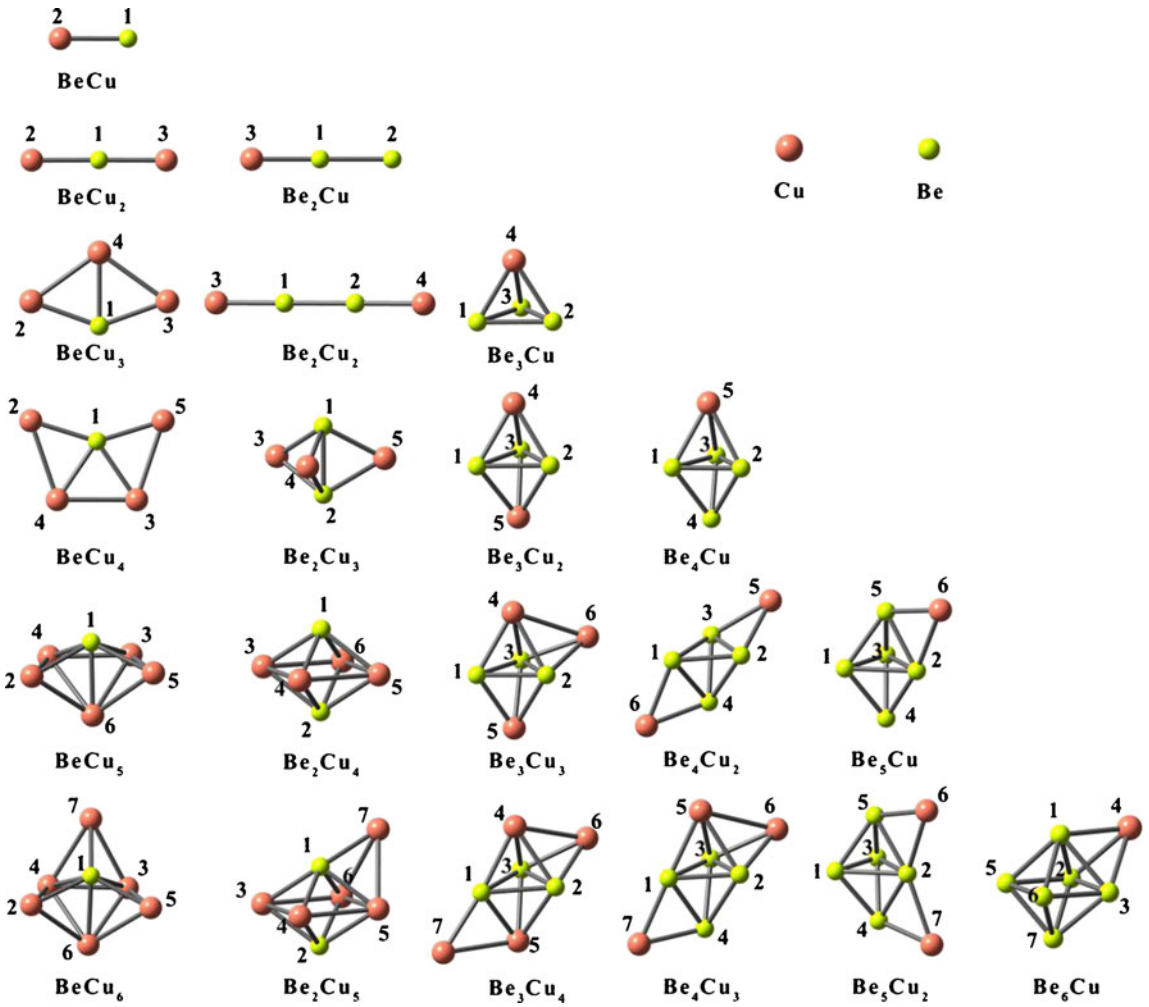

Fig. 1 The lowest energies structures of the Be_nCu_m clusters (n+m=2–7)

Table 2 The symmetries and lowest vibrational frequencies (ν_1, cm^{-1}) of the Be_nCu_m ($n+m$=2–7) clusters

Clusters	Symmetry	ν_1	Clusters	Symmetry	ν_1
BeCu	$C_{\infty v}$	481	Be_3Cu	C_s	164
$BeCu_2$	$D_{\infty h}$	167	Be_3Cu_2	D_{3h}	184
$BeCu_3$	C_{2v}	126	Be_3Cu_3	C_s	64
$BeCu_4$	C_{2v}	60	Be_3Cu_4	C_s	49
$BeCu_5$	C_s	56	Be_4Cu	C_{3v}	242
$BeCu_6$	C_{3v}	52	Be_4Cu_2	D_{2d}	75
Be_2Cu	$C_{\infty v}$	147	Be_4Cu_3	C_s	82
Be_2Cu_2	$D_{\infty h}$	75	Be_5Cu	C_s	100
Be_2Cu_3	D_{3h}	40	Be_5Cu_2	C_{2v}	86
Be_2Cu_4	D_{4h}	86	Be_6Cu	C_{3v}	209
Be_2Cu_5	C_s	60			

For Be_2Cu_2 with $D_{\infty h}$ symmetry, the Be-Be bond length is 2.122 Å, and the Be-Cu distance is 2.048 Å. The addition of one more Cu atom to $BeCu_2$ generates the first 3D configuration in this series. Be_2Cu_3 has a D_{3h} geometry. The next one in this group is Be_2Cu_4 with D_{4h} symmetry. It can be viewed as one copper atom inserts in the Cu_3 plane of Be_2Cu_3, which leads to the Cu-Cu bond formation but breaks the bond between two Be atoms. The Be_2Cu_5 cluster, with C_s spatial symmetry, could be regarded as one copper atom bound to the "hollow" site of the Be_2Cu_4 configuration, as is clearly shown in Fig. 1. From Table 3, the Be-Cu and Cu-Cu bond lengths of Be_2Cu_5 vary in the range of 2.131~2.175 Å and 2.492~2.572 Å, respectively.

In the Be_2Cu_m series, the Be-Cu bond length has an increasing tendency with increasing number of Cu atom, whereas the

Table 3 The bond lengths of the Be_nCu_m ($n+m$=2–7) clusters in their lowest energy configurations

Cluster	Type	L/Å	Cluster	Type	L/Å	Cluster	Type	L/Å
BeCu	1–2	2.057		2–6	2.175	Be_4Cu_2	1–4	1.971
$BeCu_2$	1–2	2.044		3–4	2.537		3–4	2.074
$BeCu_3$	1–2	2.093		3–6	2.572		4–6	2.143
	1–4	2.126		5–6	2.492	Be_4Cu_3	1–2	2.104
	2–4	2.426		6–7	2.570		1–4	2.033
$BeCu_4$	1–2	2.080	Be_3Cu	1–2	1.986		1–5	2.195
	1–4	2.119		2–3	2.230		1–7	2.129
	3–4	2.381		1–4	2.252		2–3	2.010
	3–5	2.499		2–4	2.126		2–4	2.182
$BeCu_5$	1–2	2.129	Be_3Cu_2	2–3	2.168		2–5	2.197
	1–4	2.142		2–4	2.134		2–6	2.172
	1–6	2.187	Be_3Cu_3	1–2	2.113		4–7	2.145
	3–4	2.409		1–4	2.160		5–6	2.614
	3–5	2.516		1–5	2.109	Be_5Cu	1–3	2.026
	3–6	2.493		2–3	2.125		2–3	2.177
	5–6	2.411		2–4	2.155		2–4	2.036
$BeCu_6$	1–2	2.114		2–5	2.194		2–5	2.000
	1–4	2.215		2–6	2.177		2–6	2.220
	2–6	2.485		4–6	2.573		3–4	2.013
	3–6	2.417	Be_3Cu_4	1–2	2.187		3–5	2.081
Be_2Cu	1–2	2.160		1–4	2.185		5–6	2.122
	1–3	2.044		1–5	2.066	Be_5Cu_2	1–3	1.884
Be_2Cu_2	1–2	2.122		1–7	2.110		2–3	2.226
	1–3	2.048		2–3	2.101		2–4	2.022
Be_2Cu_3	1–2	2.014		2–4	2.152		2–6	2.240
	1–3	2.131		2–5	2.221		3–4	2.041
Be_2Cu_4	1–3	2.153		2–6	2.183		5–6	2.118
	4–5	2.517		4–6	2.515	Be_6Cu	1–3	2.085
Be_2Cu_5	1–3	2.172		5–7	2.510		1–4	2.203
	1–6	2.147	Be_4Cu	2–3	2.045		1–6	2.076
	1–7	2.140		2–4	2.032		5–6	1.993
	2–3	2.131		2–5	2.178			

Be-Be bond length behaves reversely. For example, the Be1-Cu3 bond length increases in the order 2.044 Å for Be_2Cu< 2.048 Å for Be_2Cu_2<2.131 Å for Be_2Cu_3<2.153 Å for Be_2Cu_4 <2.172 Å for Be_2Cu_5. Differently, the Be-Be bond length shows a decreasing order of 2.160 Å for Be_2Cu>2.122 Å for Be_2Cu_2>2.014 Å for Be_2Cu_3. Although the two Be atoms do not bond together in the last two clusters, adding a Cu atom to Be_2Cu_4 shortens the Be-Be distance to 2.380 Å from 2.421 Å.

3. *Be_3Cu_m* (*m=1–4*). From Fig. 1, all the clusters in this series prefer 3D configurations. In each cluster, the three Be atoms bond to each other and construct a triangle, which is surrounded by additional Cu atoms. In the case of Be_3Cu, the Be2-Cu4 bond of 2.126 Å is 0.126 Å shorter than the Be1-Cu4 bond, and the Be1-Be2 bond of 1.986 Å is 0.244 Å shorter than the Be2-Be3 bond. Consequently, Be_3Cu has a C_s geometrical symmetry. The Be_3Cu_2 cluster has a trigonal-bipyramidal geometry. From Table 3, the Be-Cu and Be-Be bond lengths of Be_3Cu_2 are 2.134 Å and 2.168 Å, respectively. Cu-Cu bond forms in the Be_3Cu_3 and Be_3Cu_4 clusters. The Cu-Cu bond length of Be_3Cu_3 is 2.573 Å, which is ca. 0.06 Å longer than those of Be_3Cu_4.

It is noteworthy that each structure of the Be_3Cu_m series could be viewed as a Cu atom attaching to that of Be_3Cu_{m-1}. Specifically, Be_3Cu_2 could be viewed as a Cu atom capping the Be3 unit of Be_3Cu; similarly, Be_3Cu_3 could be regarded as a Cu atom occupying the "hollow" site of Be_3Cu_2. The same rule is true for the Be_3Cu_4 cluster, which could be treated as a Cu atom side-bound to the Be_3Cu_3 structure. Generally, the Be-Cu bond tends to become longer with the increasing number of *m*. From Table 3, the Be2-Cu4 bond length increases in the sequence 2.126 Å for Be_3Cu< 2.134 Å for Be_3Cu_2<2.155 Å for Be_3Cu_3≈2.152 Å for Be_3Cu_4. On the contrary, the Be-Be bond varies in a decreasing order. Take Be2-Be3 bond length for example, it decreases in the order 2.230 Å (Be_3Cu)>2.168 Å (Be_3Cu_2) >2.125 Å (Be_3Cu_3)>2.101 Å (Be_3Cu_4).

4. *Be_4Cu_m* (*m=1–3*). A previous work has specified the tetrahedral arrangement of the atoms in the singlet spin-multiplicity state as the most stable isomer of Be_4 [29]. In the Be_4Cu_m series, it is obviously seen that all the configurations could be obtained by attaching copper atoms to the bare tetrahedral Be_4 cluster. Herein, the C_{3v}-symmetrical Be_4Cu could be viewed as a copper atom capping one face of Be_4 tetrahedron. The Be-Be bond lengths are 2.032 and 2.045 Å, for bond 2–4 and bond 2–3, respectively; the Be-Cu bond length is 2.178 Å. Two Cu atoms attached to the opposite sides of the Be_4 cluster generates the D_{2d} geometry of Be_4Cu_2, where the Be-Cu bond length of 2.143 Å is slightly shorter than that of Be_4Cu. The final cluster in this group is Be_4Cu_3 with C_s group point symmetry. From Fig. 1, this cluster could be regarded as a Cu atom capping the Be1-Be2-Be3 face of Be_4Cu_2, or could be viewed as two copper atoms being attached to Be_4Cu on two different edges. From Table 3, the Be-Cu and Be-Be bond lengths of Be_4Cu_3 vary in the 2.129~2.197 Å and 2.010~2.182 Å ranges, respectively. The Cu-Cu bond emerges in this configuration and its length is 2.614 Å.
5. *Be_5Cu_m* (*m=1*, *2*). As previously reported by Srinivas et al., the most stable structure of the pure Be_5 cluster is a trigonal bipyramid (D_{3h}) [29]. From Fig. 1, both Be_5Cu and Be_5Cu_2 clusters could be generated by adding the Cu atoms to the Be_5 configuration. Herein, C_{2v}–symmetrical Be_5Cu_2 could also be regarded as a Cu atom attaching to Be_5Cu without Cu-Cu bond formation. The introduction of a second Cu atom to Be_5Cu leads to slightly longer Be2-Cu6 bond and meanwhile reduces the Be5-Cu6 bond to a small extent. Such changes in Be-Cu bond lengths imply a "repulsion" interaction between two Cu atoms in Be_5Cu_2. This special phenomenon can also be discerned in structures of the $BeCu_2$, Be_2Cu_2, Be_3Cu_2, and Be_4Cu_2 clusters, where the two Cu atoms always locate as far as possible from each other. Also note from these Be_nCu_2 series that the Be-Cu bond length shows an increasing tendency with the increasing number of Be atom. From Table 3, the Be-Cu bond length varies in the order 2.044 Å for $BeCu_2$<2.048 Å for Be_2Cu_2< 2.134 Å for Be_3Cu_2<2.143 Å for Be_4Cu_2<2.179 Å (average length of two Be-Cu bonds) for Be_5Cu_2. This may indicate that the strength of Be-Cu bond becomes weaker with increasing proportion of Be in these clusters.
6. *Be_6Cu*. Since the structure of the most stable isomer of Be_6 is reported as an O_h octahedron in the quintet state [29], we have considered the different spin multiplicity of Be_6Cu. It turns out that the global minimum of Be_6Cu corresponds to the quartet state, with a capped octahedral geometry (C_{3v}). In contrast, the doublet spin-multiplicity state of Be_6Cu is a low-lying structure, which is 0.23 eV higher in total energy than the quartet isomer. From Fig. 1, the structure of Be_6Cu could be obtained by adding a Cu atom to that of pure Be_6 cluster.

Based on the above descriptions, the global minima of these binary clusters prefer the core-shell structures, and this trend becomes more and more evident with the increasing size of the cluster. The Be atoms tend to gather together and act as the central core of these Be_nCu_m clusters, which consequently yields a maximum of Be-Be bonds. On the other hand, there is a tendency for Cu atoms to segregate toward the Be_n cluster surface, which may be due

to the relatively large Cu atomic radius. As a result, all the Be_nCu_m ($n \geq 3$) clusters could be generated by attaching Cu atoms to bare Be_n clusters. Besides, the additional Cu atoms tend to favor the "hollow" or "edge" site of the Be_n geometry.

The structural features of these binary Be-Cu clusters are also related to those of pure Be_n and Cu_m clusters. It has been reported that the copper clusters (Cu_m) favor planar configurations when $m<7$[53], while the Be_n geometries are 3D from $n=4$ onward [29]. Similar to the Cu_m cluster, $BeCu_m$ ($m<5$) have planar structures. However, the doped Be atom leads to a tridimensional geometry of $BeCu_m$ at $m=5$. As the number of Be atoms increases in the systems, the 3D structures are favored as in pure beryllium clusters. Furthermore, the greater proportion of Be in these clusters, the earlier the 3D structure occurs. From Fig. 1, the 3D configuration emerges when the total atoms number $k=6$ ($k=n+m$) in the first $BeCu_m$ series, while it occurs at $k=5$ and $k=4$ in the following Be_2Cu_m and Be_3Cu_m series, respectively.

To further reveal the origin of the structural characteristics of these binary clusters, the average coordination numbers (Nc) of Be and Cu atoms in Be_nCu_m are introduced, which can be defined as

$$average\ Nc(Be) = (2 \times N_{Be-Be} + N_{Be-Cu})/n;$$
$$average\ Nc(Cu) = (2 \times N_{Cu-Cu} + N_{Be-Cu})/m,'$$

where $N_{Be\text{-}Be}$, $N_{Cu\text{-}Cu}$, and $N_{Be\text{-}Cu}$ represent the numbers of Be-Be, Cu-Cu, and Be-Cu bonds in the binary Be_nCu_m clusters, respectively. Herein, the structures of the pure Be_n and Cu_m clusters are obtained from the previous works [29, 37, 40, 53] and reoptimized at the B3PW91 level (with the SDD basis set for Cu and aug-cc-pVTZ for Be). The relationships between average Nc's and n and m are plotted in Fig. 2. From Fig. 2, we can easily note that Nc(Cu) is smaller than Nc(Be) for most Be_nCu_m clusters. Consequently, among the 21 Be_nCu_m configurations, except for six clusters which are 1D and 2D, the other conformers favor 3D structures due to the trend toward the higher Nc for Be atoms.

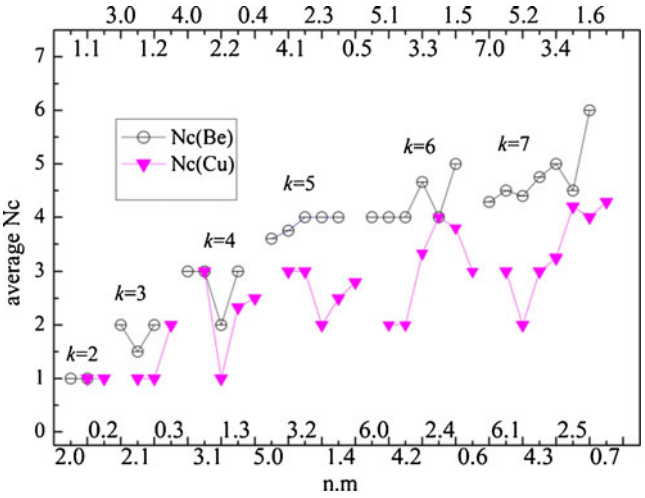

Fig. 2 Average coordination numbers (Nc) in the most stable structures of neutral binary clusters, Be_nCu_m (n.m). The scale (n.m) is given in the increasing order of $k=n+m$ and the increasing order of m for the given k [(2.0), (1.1), (0.2); (3.0), (2.1), (1.2), (0.3); … (0.7)]. It can be seen that Nc(Cu) tends to be smaller than Nc(Be)

Electronic properties and relative stabilities

The relative stabilities of different sized Be_nCu_m clusters can be represented by the cohesive energies, the successive binding energies, and the second difference of the total energy.

The cohesive energies (E_C) of the Be_nCu_m clusters are calculated according to equation (1), the results are presented in Fig. 3.

$$E_C = [nE(Be) + mE(Cu) - E(Be_nCu_m)]/(n+m) \quad (1)$$

From Fig. 3a, the cohesive energy data do not yield a monotonic variation. In the curves, the peaks occur when the number of copper atoms is even. For instance, the peak emerges at $BeCu_2$ for $k=3$, at Be_3Cu_2 for $k=5$, at Be_2Cu_4 for $k=6$, and at Be_3Cu_4 for $k=7$. There is an exception for $k=4$, that is, the E_C value of $BeCu_3$ is the highest (1.317 eV). Nevertheless, it can be seen from the figure that the Be_2Cu_2 cluster also has a high E_C, which is only 0.017 eV less than that of $BeCu_3$. Since the clusters corresponding to the peaks possess relative higher cohesive energies, they may be more difficult to be broken than their neighboring ones. In addition, we have calculated the average cohesive energies (average E_C) for the given k and plotted the results in Fig. 3b. From the figure, the average E_C value increases monotonically with the number of k. In addition, it rises sharply from $k=2$–5, then increases smoothly from $k=5$–7. Therefore, the average cohesive energies of the Be_nCu_m species show a tendency to reach a constant value from $k=5$ onward.

Figure 4 shows the successive binding energies (sBE_{Cu}) of these binary clusters, which are defined as

$$(sBE)_{Cu} = E[Be_nCu_m - 1] + E[Cu] - E[Be_nCu_m]$$

In the figure, both the sBE_{Cu} curves for the $BeCu_m$ ($m=1$–6) and Be_2Cu_m ($m=1$–5) series exhibit pronounced odd-even oscillatory behavior. Particularly prominent sBE peaks are found at $m=2$, 4, 6 for the $BeCu_m$ clusters, and the peaks occur at $m=2$, 4 among the Be_2Cu_m series, suggesting that the clusters containing even Cu atoms have relative higher stabilities as compared with their neighbors. The Be_2Cu_4 cluster exhibits the largest sBE_{Cu} value of 2.960 eV, implying its stability with respect to loss of Cu atom.

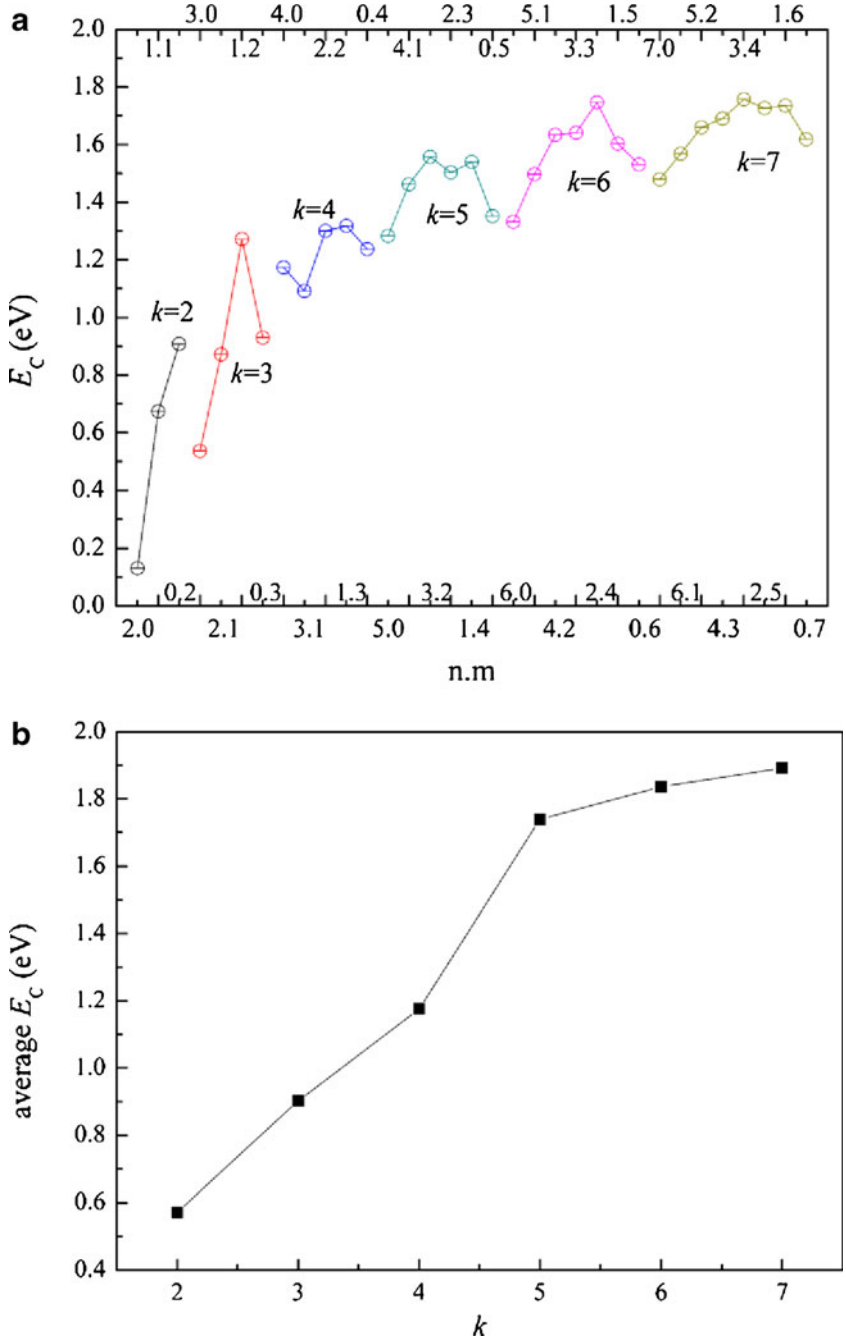

Fig. 3 **a** The cohesive energies (E_C) of the most stable structures of the Be_nCu_m (n.m) binary clusters. The scale (n.m) is given in the increasing order of $k=n+m$ and the increasing order of m for the given k [(2.0), (1.1), (0.2); (3.0), (2.1), (1.2), (0.3); … (0.7)]. **b** Average cohesive energies (average E_C) for the given k

The second difference energy is a sensitive quantity to evaluate the relative stability of the clusters, which can be defined as

$$\Delta^2 E[BeCu_m] = E[BeCu_{m-1}] + E[BeCu_{m+1}] - 2E[BeCu_m]$$

$\Delta^2 E[BeCum]$ represents a comparison between two fragmentation processes: $BeCu_{m+1} \rightarrow BeCu_m + Cu$ and $BeCu_m \rightarrow BeCu_{m-1} + Cu$. Positive $\Delta^2 E$ value indicates that the dissociation of $BeCu_{m+1}$ into $BeCu_m$ is a more favorable process than the fragmentation of $BeCu_m$ into $BeCu_{m-1}$. Therefore $\Delta^2 E > 0$ means that the $BeCu_m$ clusters are particularly stable. The $\Delta^2 E$ values of the $BeCu_m$ clusters are calculated and shown in Fig. 5. From Fig. 5, $\Delta^2 E$ presents a clear odd-even alternation again, with peaks (bottoms) at an even (odd) number of copper atoms. Positive values are presented for $BeCu_2$ (1.01 eV) and $BeCu_4$ (0.50 eV). The largest $\Delta^2 E$ value for $BeCu_2$ indicates its high stability. Based on the above analyses, $BeCu_2$ exhibits the highest relative stability among the Be_nCu_m clusters and may be used as the building block for novel cluster-assembled materials due to its large electronic properties and special stability.

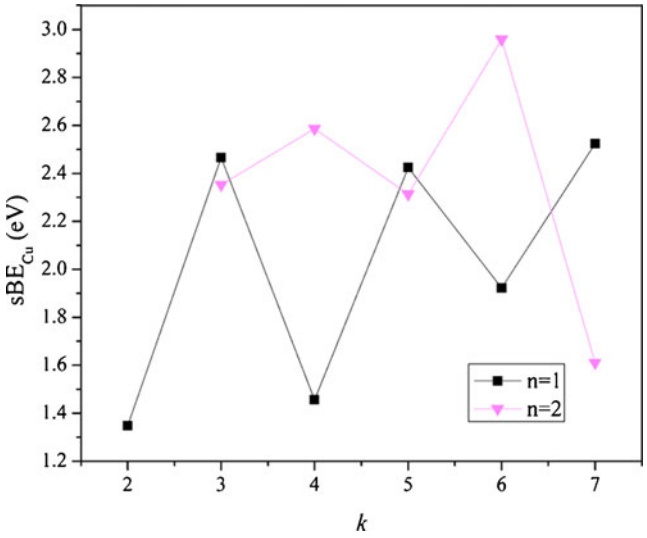

Fig. 4 Successive binding energies (sBE$_{Cu}$) for the $BeCu_m$ and Be_2Cu_m clusters

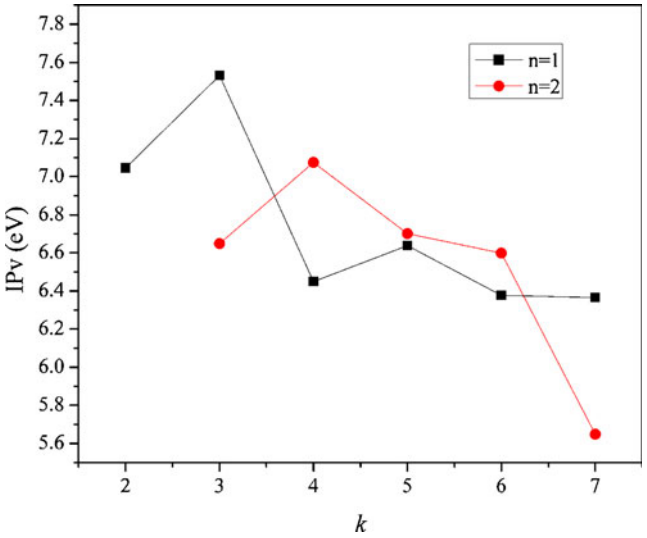

Fig. 6 The vertical ionization potentials (IP$_v$) of the $BeCu_m$ and Be_2Cu_m clusters

The stabilities of these Be_nCu_m clusters can also be discussed on the basis of the vertical ionization potentials (IP$_v$), HOMO-LUMO gaps, and chemical hardness.

The vertical ionization potential (IP$_v$) is considered to be an important criterion for evaluating the stability of clusters. It is defined as the total energy difference between the neutral cluster and the ionized cluster with the same geometry as the neutral. Based on the calculation results, the IP$_v$ values of the Be_nCu_m clusters are extremely large (5.524–7.685 eV), implying that all these clusters are difficult to lose an electron. The IP$_v$ data of the $BeCu_m$ and Be_2Cu_m series are shown in Fig. 6, as a function of the total atoms number *k*. And there are two features that can be noted from these curves: (1) they all show even-odd oscillation behaviors as *m* increases; (2) in general, the IP$_v$ value decreases as the cluster size increases.

The gap between the highest occupied molecular orbital (HOMO) and the lowest unoccupied molecular orbital (LUMO) is an effective measurement for assessing the stability of clusters. The HOMO-LUMO energy gap reflects the ability for electrons to jump from occupied molecular orbital to unoccupied molecular orbital, which indicates the ability of a molecule to participate in chemical reaction to some degree. The gap values of the $BeCu_m$ and Be_2Cu_m clusters are presented in Fig. 7. It is worthwhile to note that the peak occurring at $BeCu_2$ is especially prominent, which indicates that the $BeCu_2$ cluster is relatively more stable than the other ones. Among the Be_2Cu_m series, the largest HOMO-LUMO gap value of Be_2Cu_2 suggests its high stability.

We have also calculated the chemical hardness for these Be_nCu_m clusters. With the knowledge of the ionization

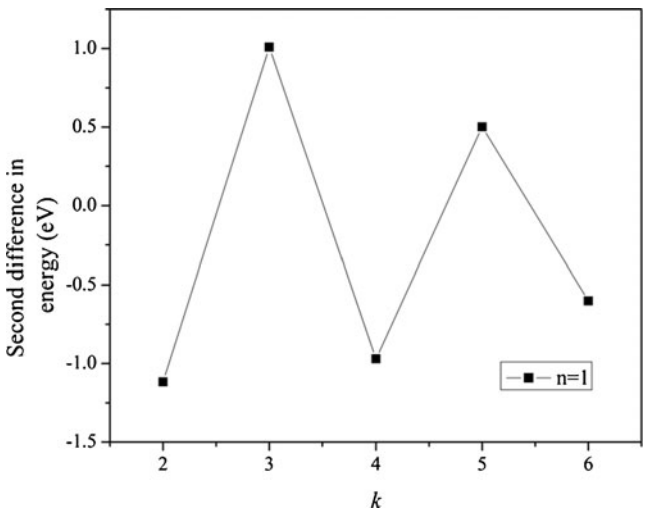

Fig. 5 Second difference in energy (in eV) of the $BeCu_m$ clusters

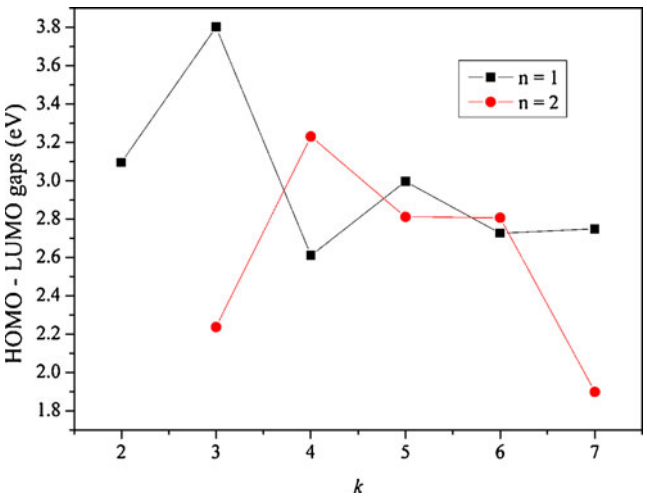

Fig. 7 HOMO–LUMO gap (in eV) of the $BeCu_m$ and Be_2Cu_m clusters

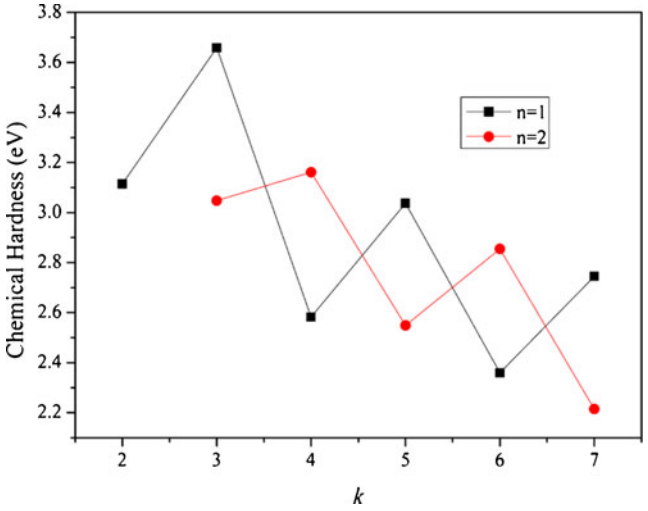

Fig. 8 Chemical hardness (in eV) of the $BeCu_m$ and Be_2Cu_m clusters

potential and the electron affinity, it is possible to calculate the global chemical hardness (η) [58] which can be approximated as,

$$\eta \doteq \frac{1}{2}(I - A)$$

where I and A are the vertical ionization potential and the electron affinity, respectively. Structures with large hardness values are often considered to be harder, namely, less reactive and more stable. The chemical hardness data of the $BeCu_m$ and Be_2Cu_m clusters are shown in Fig. 8. From the figure, each curve shows visible odd-even oscillation and the chemical hardness values of the even valence electron clusters are larger than those of their neighboring clusters. Herein, $BeCu_2$ possesses the largest hardness of 3.66 eV and Be_2Cu_2 is second to $BeCu_2$. Actually, no matter in which series, the cluster with two copper atoms exhibits the highest chemical hardness value.

At last, we performed the natural population analysis of these binary clusters. There is an interesting phenomenon that the charge-transfer direction may be changed when the size of the $ZrSi_n$ clusters increases [59]. This change also happens in Be-doped gold clusters [60, 61]. Note that the same is true for the Be_nCu_m clusters. From Table 4, the beryllium atoms possess charges ranging from −1.438e to 0.180e and the charge-transfer direction changes at $BeCu_3$, Be_2Cu_3, and Be_3Cu_2 for the $BeCu_m$ (m=1–6), Be_2Cu_m (m=1–5), and Be_3Cu_m (m=1–4) series, respectively. In a previous work, Rodriguez and Goodman had demonstrated that, in bimetallic systems involving species with similar electron donor-electron acceptor properties, the subtle balance that determines the flow of charge between elements can be easily affected by changes in the coordination number or in the geometrical arrangement of the atoms [62]. For the investigated Be_nCu_m clusters, the average coordination number of Be atom is also shown in Table 4. From the table,

Table 4 The natural charge populations and the coordination number of Be atoms of the Be_nCu_m clusters

Cluster	Nc(Be)	Be total	Cu-1	Cu-2	Cu-3	Cu-4	Cu-5	Cu-6
BeCu	1	0.158	−0.158					
$BeCu_2$	2	0.072	−0.036	−0.036				
$BeCu_3$	3	−0.252	0.112	0.112	0.029			
$BeCu_4$	4	−0.752	0.209	0.209	0.167	0.167		
$BeCu_5$	5	−0.947	0.308	0.308	0.205	0.205	−0.080	
$BeCu_6$	6	−1.438	0.388	0.388	0.388	0.091	0.090	0.090
Be_2Cu	1.5	0.070	−0.070					
Be_2Cu_2	2	0.180	−0.090	−0.090				
Be_2Cu_3	4	−0.900	0.300	0.300	0.300			
Be_2Cu_4	4	−0.712	0.178	0.178	0.178	0.178		
Be_2Cu_5	4.5	−1.208	0.311	0.219	0.184	0.311	0.184	
Be_3Cu	3	0.015	−0.015					
Be_3Cu_2	4	−0.310	0.155	0.155				
Be_3Cu_3	4.67	−0.648	0.290	0.290	0.088			
Be_3Cu_4	5	−0.870	0.256	0.215	0.201	0.197		
Be_4Cu	3.75	−0.203	0.203					
Be_4Cu_2	4	−0.502	0.251	0.251				
Be_4Cu_3	4.75	−0.822	0.326	0.265	0.231			
Be_5Cu	4	−0.283	0.283					
Be_5Cu_2	4.4	−0.384	0.192	0.192				
Be_6Cu	4.5	−0.335	0.335					

the charges transfer from Be atoms to Cu atoms when Nc(Be) is less than 3, and the direction of charge flow reverses when Nc(Be) > 3. Hence, the average coordination numbers of Be atom may be the key factor influencing the charge transfer in the Be_nCu_m clusters.

Conclusions

In summary, we have extensively investigated the neutral Be_nCu_m ($n+m=2–7$) bimetal clusters by DFT theory employing the B3PW91 functional. We find several interesting structural features for these binary clusters, which may serve as useful guidelines for determining the most stable structures of the larger binary Be-Cu clusters. The main observations are as follows:

1. In the most stable structures, the Be atoms tend to gather together and occupy the highest coordinated sites. Meanwhile, there is a tendency for Cu atoms to segregate toward the Be_n cluster surface. Such configurations prefigure the core-shell form of larger Be-Cu nanoclusters.
2. The calculation results of IP_v, HOMO-LUMO gaps, chemical hardness, second difference energies and sBE all present odd-even alternations. The stability analyses based on the energies and the physical properties clearly show that the clusters with even number of copper atoms are more stable than the others. Particularly, the linear $BeCu_2$ configuration exhibits special stability among the Be_nCu_m clusters.
3. According to the natural population analysis (NPA), we find that when the average coordination number of Be atom in the Be_nCu_m clusters are less than 3, the charge transfers from Be to Cu, but when the Nc(Be) increases, the charges transfer from copper atoms to beryllium.

Acknowledgments This work was supported by the National Natural Science Foundation of China (Grant No. 21173095).

References

1. Yu S, Jia X, Dong L, Yin Y (2011) Structures of small Fe(n-1)Ni(*n*=2–7) clusters: a density funcational theory study. Asian J Chem 23(4):1854–1856
2. Molayem M, Grigoryan VG, Springborg M (2011) Theoretical determination of the most stable structures of Ni(m)Ag(n) bimetallic nanoalloys. J Phys Chem C 115(15):7179–7192. doi:10.1021/jp1094678
3. Karagiannis EE, Kefalidis CE, Petrakopoulou I, Tsipis CA (2011) Density functional study of structural, electronic, and optical properties of small bimetallic ruthenium-copper clusters. J Comput Chem 32(7):1241–1261. doi:10.1002/jcc.21705
4. Venkataramanan NS, Sahara R, Mizuseki H, Kawazoe Y (2010) Titanium-doped nickel clusters TiNi(n) (*n*=1–12): geometry, electronic, magnetic, and hydrogen adsorption properties. J Phys Chem A 114(15):5049–5057. doi:10.1021/jp100459c
5. Kilimis DA, Papageorgiou DG (2010) Density functional study of small bimetallic Ag-Pd clusters. J Mol Struc-Theochem 939(1–3):112–117. doi:10.1016/j.theochem.2009.09.048
6. Kilimis DA, Papageorgiou DG (2010) Structural and electronic properties of small bimetallic Ag-Cu clusters. Eur Phys J D 56(2):189–197. doi:10.1140/epjd/e2009-00295-1
7. Merritt JM, Bondybey VE, Heaven MC (2008) Experimental and theoretical study of the electronic spectrum of BeAl. Phys Chem Chem Phys 10(35):5403–5411. doi:10.1039/b806879h
8. Jiang ZY, Lee KH, Li ST, Chu SY (2006) Structures and charge distributions of cationic and neutral Cun-1Ag clusters (n=2–8). Phys Rev B doi:10.1103/PhysRevB.73.235423
9. Ferrando R, Fortunelli A, Rossi G (2005) Quantum effects on the structure of pure and binary metallic nanoclusters. Phys Rev B doi:10.1103/PhysRevB.72.085449
10. Fernandez EM, Soler JM, Garzon IL, Balbas LC (2004) Trends in the structure and bonding of noble metal clusters. Phys Rev B doi:10.1103/PhysRevB.70.165403
11. Baletto F, Mottet C, Rapallo A, Rossi G, Ferrando R (2004) Growth and energetic stability of AgNi core-shell clusters. Surf Sci 566:192–196. doi:10.1016/j.susc.2004.05.044
12. Lee HM, Ge MF, Sahu BR, Tarakeshwar P, Kim KS (2003) Geometrical and electronic structures of gold, silver, and gold-silver binary clusters: Origins of ductility of gold and gold-silver alloy formation. J Phys Chem B 107(37):9994–10005. doi:10.1021/jp034826+
13. Gaudry M, Cottancin E, Pellarin M, Lerme J, Arnaud L, Huntzinger JR, Vialle JL, Broyer M, Rousset JL, Treilleux M, Melinon P (2003) Size and composition dependence in the optical properties of mixed (transition metal/noble metal) embedded clusters. Phys Rev B doi:10.1103/PhysRevB.67.155409
14. Dennler S, Ricardo-Chavez JL, Morillo J, Pastor GM (2003) Density functional calculations on small bimetallic magnetic clusters. Eur Phys J D 24(1–3):237–240. doi:10.1140/epjd/e2003-00130-9
15. Borin AC, Rodrigues ALG (2003) The lowest-lying electronic states of BeMg. Chem Phys Lett 372(5–6):698–707. doi:10.1016/s0009-2614(03)00483-4
16. Fournier R (2001) Theoretical study of the structure of silver clusters. J Chem Phys 115(5):2165–2177. doi:10.1063/1.1383288
17. Derosa PA, Seminario JM, Balbuena PB (2001) Properties of small bimetallic Ni-Cu clusters. J Phys Chem A 105(33):7917–7925. doi:10.1021/jp0104637
18. Sanchez-Castro ME, Sanchez-Vazquez M (2011) Structure and reactivity of Be(n) cycles (*n*=3–12): A DFT study. Computational and Theoretical Chemistry 967(1):136–139. doi:10.1016/j.comptc.2011.04.006
19. Heaven MC, Merritt JM, Bondybey VE (2011) Bonding in beryllium clusters. Annu Rev Phys Chem doi:10.1146/annurev-physchem-032210-102545
20. Heaven MC, Bondybey VE, Merritt JM, Kaledin AL (2011) The unique bonding characteristics of beryllium and the Group IIA metals. Chem Phys Lett 506(1–3):1–14. doi:10.1016/j.cplett.2011.02.025
21. Ascik PN, Wilke JJ, Simmonett AC, Yamaguchi Y, Schaefer HF, III (2011) The Beryllium tetramer: profiling an elusive molecule. J Chem Phys doi:10.1063/1.3553366
22. Schmidt MW, Ivanic J, Ruedenberg K (2010) Electronic structure analysis of the ground-state potential energy curve of Be(2). J Phys Chem A 114(33):8687–8696. doi:10.1021/jp101506t
23. Antonov IO, Barker BJ, Bondybey VE, Heaven MC (2010) Spectroscopic characterization of Be(2)(+) X (2)Sigma(+)(u) and the ionization energy of Be(2). J Chem Phys doi:10.1063/1.3472977

24. Merritt JM, Bondybey VE, Heaven MC (2009) Beryllium dimercaught in the act of bonding. Science 324(5934):1548–1551. doi:10.1126/science.1174326
25. Merritt JM, Kaledin AL, Bondybey VE, Heaven MC (2008) The ionization energy of Be(2), and spectroscopic characterization of the (1)(3)Sigma(+)(u), (2)(3)Pi(g), and (3)(3)Pi(g) states. Phys Chem Chem Phys 10(27):4006–4013. doi:10.1039/b803975e
26. Zhao Y, Li N, Xu WG, Li QS (2007) Structure and stability of Be(6), Be(6)(+), and Be(6)(−) clusters. Int J Quantum Chem 107(1):81–91. doi:10.1002/qua.21064
27. Cerowski V, Rao BK, Khanna SN, Jena P, Ishii S, Ohno K, Kawazoe Y (2005) Evolution of the electronic structure of Be clusters. J Chem Phys doi:10.1063/1.2001655
28. Zhao Y, Li S, Xu WG, Li QS (2004) Structure and stability of Be(5), Be(5)(+), and Be(5)(−) clusters. J Phys Chem A 108(22):4887–4894. doi:10.1021/jp037892k
29. Srinivas S, Jellinek J (2004) Structural and electronic properties of small beryllium clusters: a theoretical study. J Chem Phys 121(15):7243–7252. doi:10.1063/1.1791071
30. Lee JS (2003) Basis-set limit binding energies of Be-n and Mg-n (n=2,3,4) clusters. Phys Rev A 68(4). doi:10.1103/PhysRevA.68.043201
31. Kaplan IG, Roszak S, Leszczynski J (2001) Binding in clusters with closed-subshell atoms (alkaline-earth elements). Adv Quant Chem 40:257–278. doi:10.1016/s0065-3276(01)40020-7
32. Kolchin AM, Hall RW (2000) Electronic properties of small neutral and charged beryllium clusters. J Chem Phys 113(10):4083–4092. doi:10.1063/1.1288388
33. Beyer MK, Kaledin LA, Kaledin AL, Heaven MC, Bondybey VE (2000) Density functional calculations of beryllium clusters Be-n, *n*=2–8. Chem Phys 262(1):15–23. doi:10.1016/s0301-0104(00)00256-1
34. Baishya K, Idrobo JC, Ogut S, Yang M, Jackson KA, Jellinek J (2011) First-principles absorption spectra of Cu(n) (*n*=2–20) clusters. Phys Rev B 83(24). doi:10.1103/PhysRevB.83.245402
35. Hsu W-D, Ichihashi M, Kondow T, Sinnott SB (2007) Ab initio molecular dynamics study of methanol adsorption on copper clusters. J Phys Chem A 111(3):441–449. doi:10.1021/jp065669s
36. Calaminici P, Koster AM, Gomez-Sandoval Z (2007) Density functional study of the structure and properties of Cu-9 and Cu-9(−). J Chem Theo Comput 3(3):905–913. doi:10.1021/ct600358a
37. Florez E, Mondragon F, Fuentealba P (2006) Effect of Ni and Pd on the geometry, electronic properties, and active sites of copper clusters. J Phys Chem B 110(28):13793–13798. doi:10.1021/jp060521u
38. Yang ML, Jackson KA (2005) First-principles investigations of the polarizability of small-sized and intermediate-sized copper clusters. J Chem Phys 122(18). doi:10.1063/1.1891705
39. Florez E, Tiznado W, Mondragon F, Fuentealba P (2005) Theoretical study of the interaction of molecular oxygen with copper clusters. J Phys Chem A 109(34):7815–7821. doi:10.1021/jp052245+
40. Wang HY, Li CY, Tang YJ, Zhu ZH (2004) Geometry and electronic properties of Cu-n (*n*<= 9). Chinese Phys 13(5):677–681. doi:10.1088/1009-1963/13/5/018
41. Jaque P, Toro-Labbe A (2004) The formation of neutral copper clusters from experimental binding energies and reactivity descriptors. J Phys Chem B 108(8):2568–2574. doi:10.1021/jp036260v
42. Maroulis G (2003) Is the hyperpolarizability of Cu-2 negative? A study of basis set and electron correlation effects. J Phys Chem A 107(33):6495–6499. doi:10.1021/jp0352128
43. Jug K, Zimmermann B, Calaminici P, Koster AM (2002) Structure and stability of small copper clusters. J Chem Phys 116(11):4497–4507. doi:10.1063/1.1436465
44. Alonso JA (2000) Electronic and atomic structure, and magnetism of transition-metal clusters. Chem Rev 100(2):637–677. doi:10.1021/cr980391o
45. Tong J, Li Y, Wu D, Li ZR, Huang XR (2009) Low ionization potentials of binuclear superalkali B2Li11. J Chem Phys 131(16). doi:10.1063/1.3254835
46. Roy D, Corminboeuf C, Wannere CS, King RB, Schleyer PV (2006) Planar tetracoordinate carbon atoms centered in bare four-membered rings of late transition metals. Inorg Chem 45(22):8902–8906. doi:10.1021/ic060802g
47. Bera PP, Sattelmeyer KW, Saunders M, Schaefer HF, Schleyer PV (2006) Mindless chemistry. J Phys Chem A 110(13):4287–4290. doi:10.1021/jp057107z
48. Saunders M (2004) Stochastic search for isomers on a quantum mechanical surface. J Comput Chem 25(5):621–626. doi:10.1002/Jcc.10407
49. Perdew JP, Wang Y (1992) Accurate and simple analytic representation of the electron-gas correlation energy. Phys Rev B 45:13244–13249
50. Dolg M, Wedig U, Stoll H, Preuss H (1987) J Chem Phys 86:866 doi:10.1063/1.452288
51. Kant A (1964) J Chem Phys 41:1872 doi:10.1063/1.1726169
52. Doreen G. Leopold, Joe Ho, Lineberger WC (1987) Photoelectron spectroscopy of mass - selected metal cluster anions. I. Cu-n, *n*=1–10 J Chem Phys doi:10.1063/1.452170
53. Jaque P, Toro-Labbe A (2002) Characterization of copper clusters through the use of density functional theory reactivity descriptors. J Chem Phys 117(7):3208–3218. doi:10.1063/1.1493178
54. Ghouri MM, Yareeda L, Mainardi DS (2007) Geometry and stability of BenCm (*n*=1–10; *m*=1, 2, …, to 11-n) clusters. J Phys Chem A 111(50):13133–13147. doi:10.1021/jp075931c
55. Reed AE, Curtiss LA, Weinhold F (1988) Chem Rev 88:899-926
56. Reed AE, Curtiss LA, Weinhold F (1985) J Chem Phys 83:735-746
57. Frisch MJ, Trucks GW, Schlegel HB, Scuseria GE, Robb MA, Cheeseman JR, Scalmani G, Barone V, Mennucci B, Petersson GA, Nakatsuji H, Caricato M, Li X, Hratchian HP, Izmaylov AF, Bloino J, Zheng G, Sonnenberg JL, Hada M, Ehara M, Toyota K, Fukuda R, Hasegawa J, Ishida M, Nakajima T, Honda Y, Kitao O, Nakai H, Vreven T, Montgomery JA Jr, Peralta JE, Ogliaro F, Bearpark M, Heyd JJ, Brothers E, Kudin KN, Staroverov VN, Kobayashi R, Normand J, Raghavachari K, Rendell A, Burant JC, Iyengar SS, Tomasi J, Cossi M, Rega N, Millam JM, Klene M, Knox JE, Cross JB, Bakken V, Adamo C, Jaramillo J, Gomperts R, Stratmann RE, Yazyev O, Austin AJ, Cammi R, Pomelli C, Ochterski JW, Martin RL, Morokuma K, Zakrzewski VG, Voth GA, Salvador P, Dannenberg JJ, Dapprich S, Daniels AD, Farkas Ö, Foresman JB, Ortiz JV, Cioslowski J, Fox DJ (2009) Gaussian 09, Revision A01. Gaussian, Inc, Wallingford
58. Parr RG, Pearson RG (1983) Absolute hardness: Companion parameter to absolute electronegativity. J Am Chem Soc 105:7512–7516
59. Zhao RN, Han JG, Bai JT, Sheng LS (2010) The medium-sized charged YbSi(n)(+/−) (*n*=7–13) clusters: A relativistic computational investigation. Chem Phys 378(1–3):82–87. doi:10.1016/j.chemphys.2010.10.007
60. Shao P, Kuang XY, Zhao YR, Li YF, Wang SJ (2012) Equilibrium geometries, stabilities, and electronic properties of the cationic AunBe+(*n*=1–8) clusters: Comparison with pure gold clusters. J Mol Model 18(8):3553–3562. doi:10.1007/s00894-012-1365-8
61. Chen DD, Kuang XY, Zhao YR, Shao P, Li YF (2011) Geometries, stabilities, and electronic properties of Be-doped gold clusters: a density functional theory study. Chinese Physics B doi:10.1088/1674-1056/20/6/063601
62. Rodriguez JA, Goodman DW (1992) The nature of the metal-metal bond in bimetallic surfaces. Science (New York, NY) 257(5072):897–903. doi:10.1126/science.257.5072.897